EUR 2748.e

KINETIC STUDIES OF THE EXCHANGE ADSORPTION OF IONS FROM ACID SOLUTIONS ON AN INORGANIC ION EXCHANGER

by

D. VAN DEYCK and L. H. BAETSLE

(CEN)

1966

EUR 2748.e

KINETIC STUDIES OF THE EXCHANGE ADSORPTION OF IONS
FROM ACID SOLUTIONS ON AN INORGANIC ION EXCHANGER
by D. VAN DEYCK (CEN) and L. H. BAETSLE (CEN)

European Atomic Energy Community — EURATOM
Report prepared by CEN — Centre d'Etude de l'Energie Nucléaire -
Mol (Belgium)
Euratom Contract No. 028-62-4 RISB
Brussels, February 1966 — 28 Pages — 10 Figures — FB 40

    The rate of attainment of equilibrium on ferrocyanide molybdate,
an inorganic ion exchanger simultaneously, depends on the diffusion
in the film surrounding the particle and in the solid phase itself.
A method for discernating the contributions of both mechanisms is
presented.   No explanation could be found for the discrepancy between
the experimental column capacity parameters and those derived from
theoretical considerations.

EUR 2748.e

KINETIC STUDIES OF THE EXCHANGE ADSORPTION OF IONS FROM ACID SOLUTIONS ON AN INORGANIC ION EXCHANGER

by

D. VAN DEYCK and L. H. BAETSLE
(CEN)

1966

SUMMARY

    After a short review of the main diffusion mechanisms occuring during ion-exchange reactions a thorough analysis is made of the parameters which influence the rate of attainment of equilibrium on ferrocyanide molybdate a new inorganic ion exchanger. Shallow bed runs at different flow velocity and particle size point at the fact that the overall time to reach equilibrium is divided into two parts one to be ascribed to film diffusion and the balance to particle diffusion. From the net contributions of both mechanisms the apparent diffusion coefficients are calculated showing a difference of two to three orders of magnitude between the diffusion in the film surrounding the particles and in the solid phase. Since the variability of the overall time to reach equilibrium is found to depend on the distribution coefficients another relationship is proposed for deriving the film diffusion coefficients.

    The variability observed in the particle diffusion constants of ferrocyanide molybdate on standing time in acid solution is ascribed to a degree swelling of the matrix.

    Column runs as a function of flow rate, particle size and column length show the validity of the basic assumptions used in Glueckauf's approach for the calculation of the number of theoretical plates. However, no explanation has been given for the discrepancy between the experimental column capacity parameter according to Vermeulen-Hiester's approach and the corresponding parameter in Glueckauf's theory.

KINETIC STUDIES ON THE EXCHANGE ADSORPTION OF IONS FROM ACID SOLUTIONS ON AN INORGANIC ION EXCHANGER

INTRODUCTION (✦)

The outstanding affinity of ferrocyanide molybdate (abbreviated FeMo) for Cs in acid solution has been presented in earlier papers $\underline{/}12,4\underline{/}$ together with its importance in recovery schemes of Cs^{137} from concentrated reprocessing waste solutions $\underline{/}2\underline{/}$. Compared to other inorganic ion exchangers it displays several attractive properties a.o. the easiness to prepare a granular product suited for column operations from readily available and cheap raw materials as $Na_4Fe(CN)_6$ and $NaMoO_4$.

The aim of the present article is to report on the excellent kinetic properties of the product allowing to perform column runs at high flow velocity. The implication of the fundamental kinetic theories on the selection of the optimum working conditions is analyzed with special emphasis on the diffusion mechanisms involved in the exchange reaction $Cs^+ - H$ and $Sr^{++} - H^+$. They have been proved to proceed faster than for the more common mineral ion exchangers e.a. zeolites, zirconium phosphate, resulting in shorter operation times when working with fixed bed columns. Knowing that FeMo shows trends to be dissolve when it is contacted with

highly acid (> 1M HNO_3) and neutral solutions, a high reaction rate
is a very encouraging property.

It has been tried to determine the conditions wherein the ion
exchange process is controlled by particle or film diffusion.The "shallow
bed" technique /5_/ was used for the determination of the important
diffusion or reaction constants. Several variables such as particle size,
concentration of the ions in solution and on the exchanger, flow rate,
temperature and contact time play all together a major role in the ex-
change reaction rate and have been investigated thoroughly.

Theoretical considerations

The rate of an ion exchange reaction is mainly determined by
the diffusion rate of the exchanging ions in the solid phase and through
the surrounding liquid film. Both phenomena are quite different with
respect to the way chemical equilibrium is attained between ions in
solution and in the solid phase.

A. PARTICLE DIFFUSION

If the diffusion of the exchanging ionic species in the solid
phase towards the functional groups proceeds slowly compared to the time
it takes to enter the particle surface, the rate controlling phenomenon
is called particle diffusion. BOYD /5_/, HELFFERICH et al /8, 14, 10_/
and HERING /11_/ derived general reaction rate equations specially
suited to shallow bed experiments.

HELFFERICH's approach comprises BOYD's original and more prac-
tical particle diffusion theory which may be considered as a special
case of the former when two exchanging ions have the same mobility in
the exchanger phase; such conditions prevail in isotopic exchange
reactions. Both theories differ fundamentally from each other in the
fact that BOYD suppose a constant internal diffusion coefficient
throughout the reaction, while HELFFERICH advocates a continuously

varying diffusion coefficient given by the expression :

$$\overline{D}_{AB} = \frac{\overline{D}_A \overline{D}_B (z_A^2 \overline{C}_A + z_B^2 \overline{C}_B)}{z_A^2 \overline{C}_A \overline{D}_A + z_B^2 \overline{C}_B \overline{D}_B}$$

This variable $\overline{D}_{AB}$ is called interdiffusion coefficient, to distinguish from the self diffusion coefficient $\overline{D}_A$ and $\overline{D}_B$.

In formula (1) the z_A and z_B represent the ionic valencies; $\overline{C}_A$ and $\overline{C}_B$ the relative concentrations of the ionic species in the exchanger phase.

In practice a graphical comparison of the experimental curves with theoretically calculated ones can be effected by plotting the fractional attainment of equilibrium, U (t) as a function of the logarithm of time. By sliding along the log t axis of the experimentally determined curves, till coïncidence with the theoretical calculated curves $\underline{/}$ 8,14,10,11 $\underline{}$ for a same z_A on z_B ratio it is possible to determine $\mathcal{T} = \dfrac{\overline{D}_{AB} \, t}{r_o^2}$ (2) and hence $\overline{D}_{AB}$,

whose significance will be explained below.

When normalizing, on the same kind of plot, the U (t) curves, at U (t) = 0.5, one may see that in the range $0.1 < \dfrac{\overline{D}_A}{\overline{D}_B} < 10$ the curves below U (t) $\leq$ 0.5 coincide whereas behind U (t) = 0.5 they startspreading out. At U (t) > 0.9 the spreading of the curves is considerable (see figure 1). Therefore, it is doubtfull whether one is allowed to deduce from the shape of the curves only, a quantitative information on the separate self diffusion coefficient $\overline{D}_A$ and $\overline{D}_B$ of the ions A and B in the exchanger. From these considerations it is worth mentioning that BOYD's original equations, based on a constant internal diffusion coefficient, are to be considered as an excellent practical approach of HELFFERICH's more refined theoretical curves $\underline{/}$ 10 $\underline{}$

The internal diffusion coefficient $\overline{D}_{AB}$ is usually derived from the time interval between the beginning of the reaction and the moment when it has reached 50 $°/_o$ conversion (abbreviated $t_{1/2}$). Knowing that for $0 < U$ (t) < 0.5 the normalized curves proposed by HELFFERICH and BOYD both coincide, we may choose the simple expression (3), in calculating $\overline{D}_{AB}$ from $t_{1/2}$.

$$\overline{D}_{AB} = 0.030 \ \frac{r_o^2}{t_{1/2}} \qquad (3)$$

In this formula r_o denotes the mean radius of the ion exchange particles and $\overline{D}_{AB}$ represents the mean value of $\overline{D}_{AB}$ varying according to the extent of loading throughout the whole exchange reaction. The shape of U (t) curves in the interval from 0 to 0.9 is then given within an error $< 3 \ °/_o$ by the equation (4)

$$U \ (t) = 1 - \frac{6}{\pi^2} \sum_{n=1}^{\infty} \frac{1}{n^2} \ \exp \left(- \frac{\overline{D}_{AB} \ t \ \pi^2 \ n^2}{r_o^2} \right) \qquad (4)$$

In conclusion it has to be noted that in many circumstances the feed solution is composed of a mixture of both ions A and B, instead of only one species leading at equilibrium to an incomplete conversion of the exchanger from the A into the B form. HELFFERICH's theory may be extended with only slight adjustments to such cases, provided that, the measured $\overline{D}_{AB}$ values have to be considered as mean values for the reached degree of conversion.

B. FILM DIFFUSION

When the diffusion of the exchanging ions through the liquid film of solution surrounding the ion exchanger particles is the rate determining step it is referred to as film diffusion. The exchange rate may then be described by BOYD's equation $\boxed{5}$.

$$U(t) = 1 - \exp. \left(- \frac{3\,D\,C\,t}{r_o\,\delta\,\overline{C}} \right) \qquad (5)$$

Herein D represents the diffusion coefficient of the ions in the solution, δ the film thickness; C and $\overline{C}$ the ion concentrations respectively in solution and on the exchanger.
The $t_{1/2}$ time, as explained in the preceeding paragraph and derived from equation (5) is given by :

$$t_{1/2} = 0.23 \; \frac{r_o\,\delta\,\overline{C}}{D\,C} \qquad (6)$$

To illustrate the difference in the rate of attainment of equilibrium between particle- and film diffusion, equation (5) normalized at U (t) = 0.5 is plotted together with the curves for particle diffusion control in figure 1. The graph shows an initially steeper curve for particle diffusion with a reversal at U (t) > 0.5

In the meantime several authors $\underline{/}$1, 7, 15$\underline{\smash{/}}$ have proposed some refinements by taking into account the separation factor :

$$\alpha_B^A = \frac{\overline{C}_A \cdot C_B}{\overline{C}_B \cdot C_A} \qquad (7)$$

When the two exchanging ions have equal mobilities, the analogs of equation (5) and (6) are respectively $\underline{/}$9$\underline{\smash{/}}$:

$$\ln \left(1 - U(t) \right) + \left(1 - \frac{1}{\alpha_B^A} \right) \cdot U(t) = - \frac{3\,D\,C}{r_o\,\delta\,\overline{C}\,\alpha_B^A} \cdot t \qquad (5')$$

$$\text{and } t_{1/2} = (0.167 + 0.064 \; \alpha_B^A) \cdot \frac{r_o\,\delta\,\overline{C}}{D\,C} \qquad (6')$$

As follows from expression (5) (6) (5') film diffusion depends upon several variables as there are, film thickness, particle radius and concentration of the ions in solution and on the exchanger. The influence of all these parameters shall be discussed in detail below.

Experimental

The experimental device, represented in figure 2, has been set up to follow by means of radioactive tracers the reaction rate between ions in a solution and those fixed on the ion exchanger. Similar information can also be gained from "batch" experiments. In this case a certain solution volume containing for exemple Cs^+ ions traced by Cs^{137} is contacted with an accurately weighed amount of FeMo completely in the H^+ form. The exchange of the H^+ ions with the Cs^+ ions can be computed from the decrease of the Cs^{134} radioactivity of the solution. Such reaction where the concentration of the exchanging ions in both phases are varying continuously can only be described by complicated formulas. The mathematical treatment may considerably be simplified by keeping a constant concentration of the exchanging ion in the feed solution; in the experimental set up the above requirements are met.

A small and between narrow mesh sizes quantity of ion exchange material (normally 300 mg) placed in a special reaction tube (see also figure 2) is flushed by a solution in which no measurable concentration decrease ($< 5°/_o$) of the exchanging ion occurs despite the proceeding exchange reaction. As shown on figure 2 the solution percolating at a flow rate of $\pm$ 100 ml/min, through the ion exchanger sample, is thermostatized at the desired temperature, which can be checked on the thermometer E placed just after the outlet of the reaction tube. The ion exchange material rests on a sintered glass filter closing the bottom of a small inner glass tube which slides into a reaction tube fitting in the well of a NaI crystal. The latter Y detector with its photomultiplier which is powered with a variable (from 0 to 2 KV) high tension unit, is connected through a preamplifier to a linear count ratemeter provided with a suitable recorder. When the spiked ion species in solution exchanges with the inactive one on the ion exchanger, the latter becomes increasingly radioactive as can be read on the recorder. The end point of the reaction is observed when the recorded radio-activity reaches a steady maximum. In comparing the latter radioactivity with that of an accurately pipetted volume

(normally 3 ml) of the feed solution one determines (after the necessary background corrections) the Kd value, defined as the ratio of the sorbed quantity of ions per gram of the solid phase to the concentration of the same ions per ml of the liquid phase.

The shape of the recorded curves, giving the course of attainment of equilibrium as a function of time may then be compared with those of master plots. A parameter which is further often referred to, is the already mentioned "half time", $t_{1/2}$, which is a good estimate for the reaction rate, but proves to be very sensible to a lot of variables. Potentially important parameters are for instance the mesh size of the exchanger beads, the concentration of the ions in solution, the flow rate, temperature etc. So that a quantitative characterisation of a measured reaction depends on the exact influences of all those parameters. By means of equation (3) and (6) the experimental $t_{1/2}$ times are related to the diffusion coefficients, particle size and film thicknesses.

Influence of particle size and solution flow rate on the shape of the loading curves.

It is usual to illustrate the difference between particle- and film diffusion by making a few runs using different mesh sizes,which leads to the conclusion that if the half times vary proportional to r_o^2, particle diffusion following (3) must be rate controlling. Now it can be shown that such a dependence may exist in certain cases with film diffusion too, if one assigns to the film thickness δ the empirical expression proposed by GLUECKAUF $\lfloor 6 \rfloor$:

$$ = \frac{0.2 \, r_o}{1 + 70 \, r_o \, v} \qquad (7)$$

Substituting (7) into (6') one obtains:

$$t_{1/2} = (0.0334 + 0.0128 \ \alpha_B^A) \cdot \frac{\overline{C}}{C} \cdot \frac{1}{D} \cdot \frac{r_o^2}{1 + 70 \ r_o \ v} \qquad (8)$$

In the special case of low flow rates and small particle sizes, so that $70 \ r_o \ v \ll 1$, it becomes evident that even for film diffusion a $t_{1/2}$ dependence upon r_o^2 may be encountered.

More elaborate tests for differentiating both mentioned mechanisms proved necessary. Therefore several runs have been performed on FeMo with the same aqueous solution of 10^{-3} M Sr $(NO)_3)_2$ in 0.1M HNO_3, using different mesh sizes and flow rates. The results of those numerous runs are represented only under the form of their measured $t_{1/2}$ times plotted in figure 3 versus the dimensionless parameter $\frac{1}{1 + 70 \ r_o \ v}$.

The plotted points of $t_{1/2}$ for a given mesh size in figure 3 fall quite well on straight lines, obeying equation (8).Extrapolating those lines they out the $t_{1/2}$ axis, not in the origin as should be expected from (8) if film diffusion would entirely control the reaction.

From this we may conclude that under the working conditions the diffusion phenomenon lies between film and particle diffusion. In trying to distinguish the separate parts of both mechanisms it is logical to consider the extrapolated $t_{1/2}$ times at $\frac{1}{1 + 70 \ r_o \ v} = 0$ on figure 3, as values belonging purely to particle diffusion. Indeed according to (7) δ approaches zero leaving as a first approximation a nude particle in which the ionics species caught by the surface diffuse immediately. This time can be substracted from the experimental determined $t_{1/2}$ exp. value the intrinsic film diffusion half time.

Formally this may be written down as :

$$t_{1/2}^{exp} = t_{1/2} \ (\ v = \infty) + (\ 0.0334 + 0.0128 \ \alpha_B^A) \cdot \frac{\overline{C}}{C} \frac{1}{D} \frac{r_o^2}{1 + 70 \ r_o \ v} \qquad (9)$$

denoting by $t_{1/2 \ (v = \infty)}$ the extrapolated value of $t_{1/2}$ at $\frac{1}{1+70 \ r_o \ v} = 0$ for a given range of particle radius. This value should be identical with the $t_{1/2}$ time of particle diffusion as given by equation (3):

$$t_{1/2} \ (v = \infty) = 0.030 \ \frac{r_o^2}{\overline{D}_{AB}} \qquad (3')$$

Table I shows the excellent agreement between $t_{1/2}$ ($v = \infty$) and r_o^2 ratios for different mesh sizes proving particle diffusion control.

TABLE I

Interrelationsship between the half times of the reaction $Sr^{++}-H^+$ on FeMo and the square of the particle radius.

Mesh size in ASTM	r_o^2 in $cm^2.10^4$	r_o^2 ratio	$t_{1/2(v=\infty)}$ in sec	$t_{1/2(v=\infty)}$ ratios	Slope ratios of lines in fig.3
32 - 50	4.2	6.4	160	6.9	6.9
50 - 60	1.8	2.7	65	2.8	3.0
60 - 80	1.13	1.7	45	1.9	2.3
80 -100	0.66	1	23	1	1

By differentiating (9) to $\dfrac{1}{1 + 70 \ r_o v}$ at constant r_o one obtains the slope for the straight lines in figure 3 :

$$\frac{d}{d \ (\frac{1}{1 + 70 \ r_o \ v})} \ (\ t_{1/2}^{exp} \ ) = (0.0334 + 0.0128 \ \alpha_B^A) \ \frac{\overline{C}}{C} \cdot \frac{1}{D} \cdot r_o^2 \qquad (10)$$

From (10) D may be experimentally determined. Note that following eq. (10) the slope of the lines of figure 3 would be proportional to r_o^2 as can be seen in Table I. For the considered exchange reaction $Sr^{++}- H^+$ on FeMo, the separation factor $\alpha_{Sr^{2+}}^{H^+} = 0.036$ [*] and the distribution coefficient $\dfrac{\overline{C}}{C} = 210$

[*] $\alpha_{Sr^{2+}}^{H^+}$ has been computed on the basis that in a 0.1N $Sr(NO_3)_2$ solution we found a capacity of 2.40 meq Sr/g FeMo.

and applying equation (3') and (10) one finds:

$$\bar{D}_{H^+ - Sr^{2+}} = 8.6 \quad 10^{-8} \quad cm^2/sec$$

and $\quad D_{Sr^{2+}} = 0.32 \quad 10^{-5} \quad cm^2/sec$

Due to the irregular shape of the particles those diffusion coefficients may only be considered as a good semi quantitative estimate of the true diffusion coefficient values since the listed equations were developed for spherical particles.

Influence of the partial molar concentrations of the exchanging ions in solution on the shape of the loading curves
_____

Traced solutions whose total normality of H^+ and alkali or alkaline earth metal ions equal 0.1N, are flushed at 25°C and a constant flow rate of 100 ml/min, through a sample of 300 mg FeMo, sieved between 50 and 60 mesh ASTM, completely in the H^+ form. For concentrations beneath 10^{-2} N of the metal ion in solution the recorded curves given in figure 4a, b and c bear good resemblance to those of film diffusion. By plotting the data on a log (1 - U) vs t plots, nearly straight lines are obtained. The minor deviations from linearity may be attributed to variation in the selectivity coefficient α_M^H and to the irregularities in the shape of the ion exchange particles. A still more convincing indication for film diffusion is the strong linear dependence of the $t_{1/2}$ values with the measured Kd values as shown in table II and plotted in figure 5.

Table II

Distribution coefficients and half times of the reactions
$Cs^+ - H^+$, $Rb^+ - H^+$ and $Sr^{++} - H^+$ on FeMo

Metal ion concentr. (N) x 10^2		0.01	0.05	0.1	0.5	1.0
Cs	Kd	2760	1311	800	222	-
	$t_{1/2}$ (min)	11.8	6.0	3.1	1.3	-
Rb	Kd	1098	630	431	190	-
	$t_{1/2}$ (min)	6.7	3.8	2.3	1.4	-
Sr	Kd	-	530	395	150	90
	$t_{1/2}$	-	9.5	7.2	4.5	3.1

Indeed in cases where film diffusion prevails one has to expect that, according to equation (8), the $t_{1/2}$ times should vary linearly with $\frac{\overline{C}}{C}$ or Kd providing that α_B^A is small. This has been experimentally proved on FeMo for three different kinds of ions (see figure 5). By differentiating (8) with respect to $\frac{\overline{C}}{C}$ one obtains indeed:

$$\frac{d}{d\left(\frac{\overline{C}}{C}\right)} \left(t_{1/2}\right) = (0.0334 + 0.0128 \; \alpha_B^A) \; \frac{1}{D} \; \frac{r_o^2}{1 + 70 \; r_o \; v} \qquad (11)$$

On applying equation (11), D may again be computed; some values are listed below:

$$D_{Cs^+} = 0.42 \; 10^{-5} \; cm^2/sec$$

$$D_{Rb^+} = 0.30 \; 10^{-5} \; cm^2/sec$$

$$D_{Sr^{2+}} = 0.12 \; 10^{-5} \; cm^2/sec$$

For concentrations above 10^{-2} N of the metal ions in solution, on account of the decreasing selectivity or diminishing Kd value, the recorded curves are closer to those particle diffusion. The experimental data for the Cs ion between 10^{-2} and 0.099 N are plotted on a semi log scale as shown on fig. 6 (U vs log t) which allows the comparison with theoretical curves given in fig. 1 $\underline{/}$4,8,14,10, 11$\underline{/}$. For values of U$<$0.5 those curves may be considered as belonging to the intermediate range between particle-and film diffusion processes, while above U = 0.5 their slope is still flatter than the theoretical particle diffusion curves. This indicates that whether according HELFFERICH's theory $\overline{D}_{Cs+} > 10\ \overline{D}_{H+}$, or to a serious restriction in diffusion possibilities (perhaps internal structure changes) with proceeding conversion of the ion exchangers; in figure 7 the $\overline{D}_{Cs-H}$ values varying between 1 and 6 10^{-7} cm^2/sec, are calculated from the measured $t_{1/2}$ times of the curves in figure 6, and plotted as a function of the degree of conversion $\overline{x}$ of the ion exchanger.

It is noticeable that the mean value of the interdiffusion coefficient $\overline{D}_{Cs-H}$ decreases with higher degrees of occupation of the ion exchanger with Cs. Below $\overline{x}$ = 0.5 the $\overline{D}_{Cs-H}$ cannot be plotted accurately anymore because film diffusion is predominating and as the measured $t_{1/2}^{exp}$ is due to both mechanisms. The amount of time of the parallel occuring particle diffusion mechanism becomes negligible and is therefore hardly measurable. Following HELFFERICH's theoretical conception for particle diffusion mechanisms, it would equally point at the fact that $\overline{D}_{Cs} \gg \overline{D}_{H}$. On our ion exchanger FeMo, the existing HELFFERICH's kinetic theory can hardly find an application, it nevertheless delivers some general qualitative indication about the interdiffusion coefficient variation.

The change of FeMo's kinetic behaviour upon contact time,T, with acid solution.

Previous work done on FeMo reveals a slight solubility of the exchanger in acid solutions. On account of this, the "framework" of the exchanger on which the counter ions are attached becomes more and more accessible with time. This in conjunction with the already known open structure of FeMo $\underline{/}$3$\underline{/}$ explains its fast kinetic behaviour.

To give some quantitative idea of the increasing accessibility of FeMo upon contact time, T, in acid solution, experiments were performed by means of the "fractional equilibrium" device (see above). Loadings were carried out as a function of the contact time of the sample in the solution for two different kinds of ions Cs^+ and Sr^{++} with respectively concentrations of 10^{-3} N and $0.5 \ 10^{-3}$ N in $0.1N \ HNO_3$ solutions (going from 20 min up to 15 hours).

Both series of $t_{1/2}$ measurements versus $1/_T$ are plotted in figure 8, showing that there exists a limiting value of the reaction rate even after a very long contact period.

The remarkable improvement in reaction rate behaviour with wetting may be attributed to the preparation method of FeMo involving long drying periods at 50°C (24 hours and more).

Subsequently during their solution uptake the exchanger particles swell and some of them may even break down.We have proved this swelling by measuring the fractional volume increase as a function of time see table III

TABLE III

$T =$ wetting time in min.	$T^{-1}.10^4$ min^{-1}	$t_{1/2}$ min.		V (ml) for 5g FeMo (50-60 ASTM)	ΔV (ml)	$\frac{\Delta V}{\Delta V_{Max}}$	$Bt = \tau$
		$10^{-3}N$ CsCl $0.1N$ HNO$_3$	$0.5 \ 10^{-3}N$ SrCl$_2$ $0.1N$ HNO$_3$				
0	⊖	-	-	4.82	-	-	-
20	500	10	81	5.28	0.46	0.29	0.009
30	333	10	39	5.43	0.61	0.38	0.017
60	166	6	15	5.81	0.99	0.62	0.055
120	83	4.5	8.8	5.91	1.09	0.68	0.069
300	33	3.5	5.5	6.14	1.32	0.83	0.142
900	11	3.1	5	6.41	1.59= ΔV_{Max}	1.00	1.00

Particle diffusion determines as expected the water uptake phenomenon as illustrated in figure 9 displaying also a linear $Bt = \mathcal{C}$ versus t plot.

One may therefore conclude that the studied phenomenon of swelling, accompagnied with the formation of fines (15 to $20°/_o$), is responsable for the acceleration of the reaction rates on FeMo. Hence after a certain saturation time, when all the channels are filled with solution, no further improvement in kinetic behaviour will be possible, see figure 8.

The behaviour of FeMo differs from that found for other inorganic ion exchangers with rigid structure which do not swell. Indeed the semi crystalline layered structure of FeMo $\underline{/}3\underline{\ /}$ may easily expand when contacted with acid the swelling properties of this inorganic ion exchanger resemble very much those observed for clay minerals.

Column experiments

In order to investigate the applicability of the preceeding theoretical study on ion exchange kinetics a series of runs have been performed under controlled conditions.

The variables under consideration are the particle size of the exchanger, flow rate of the saturating solution and the size of the column. The experimental conditions are summarized in table IV.

In figures 10a and 10b some breakthrough curves presented under normalized form are plotted in a prob-log diagram. Figure 10a gives for instance the dependence of the shape of the breakthrough curves upon rate of the Cs solution, while figure 10b shows the variation upon particle size for Sr. By graphical comparison with a master plot of theoretically calculated normalized curves $\underline{/}16$, $13\underline{\ /}$, the N values were determined, and given in column 6 of table IV.

Using the quantitative data of equilibrium derived from measurements of fractional attainment as there are Kd value, order of magnitude of D and/or $\overline{D}$, it should be possible to compute the breakthrough curves obtained.

From what precedes it is clear that measurements by means of the shallow bed technique provide some excellent estimation on the magnitude of the diffusion coefficients of the ions in the solution and in the exchanger phase.

GLUECKAUF $\underline{/}6\underline{_/}$ proposed an expression to calculate EHTP of a column containing the above mentioned parameters; this well known formula for the plate height H is termed as follows:

$$H = 1.64 \; r_o + \frac{\left(\frac{\overline{C}}{C}\right)}{\left(\left(\frac{\overline{C}}{C}\right) + fe\right)^2} \cdot \frac{0.14 \; r_o^2 \; v}{\overline{D}} + \left(\frac{\left(\frac{\overline{C}}{C}\right)}{\left(\frac{\overline{C}}{C}\right) + fe}\right)^2 \frac{0.266 \; r_o^2 \; v}{D \; (1+70 \; r_o \; v)} \quad (12)$$

Since in many practical experimental conditions, the column height h and the Kd (or $\frac{\overline{C}}{C}$) value are sufficiently high, to neglect the first term of (12) and neglecting fe, the following expression for N is obtained:

$$N = \frac{h}{H} = \frac{1}{r_o^2 \; v} \cdot \frac{1}{\dfrac{0.14 \; C}{\overline{C} \; \overline{D}} + \dfrac{0.266}{D \; (1 + 70 \; r_o \; v)}} \quad (13)$$

Since the factor between the brackets in the denominator of equation (13) remains approximately constant over wide ranges of r_o and v, the N values ought to vary linearly with column height, inversely proportional with the square of the particle radius and inversely proportional with the flow rate of the percolating solution.

As a matter of fact the N values are roughly proportional to the contact time of the solution per unit surface of the ion exchange material. Therefore in column experiments with a given mesh size of exchanger particles one often mentions the flow rate in column volumes per unit time.

TABLE IV

Kinetic characteristics of FeMo at 25°C for the exchange reactions:

a) $Cs^+ - H^+$ with 500 mg Cs/l in 2M HNO_3 (experiments 1 - 10)

b) $Sr^{2+} - 2H^+$ with 200 mg Sr/l in 0.2M HNO_3 (experiments 11 - 20)

1	2	3	4	5	6	7	8	9	10
N° exp.	Weight of ion exchange material (g)	Column height (h) (cm)	Mesh size ASTM	Flow rate (R) (ml/min)	N	$Nr_0^2 .10^3$ (cm^2)	N.R. (ml/min)	N/h (cm^{-1})	N calculated
1	3	3.8	32 - 50	10	11 ± 2	4.6	110	2.9	-
2	3	3.8	50 - 60	10	30 ± 4	5.4			0.26
3	3	3.8	60 - 80	10	55 ± 5	6.2			-
4	3	3.8	80 -100	10	160 ± 50	10.6			-
5	3	3.8	32 - 50	1	90 ± 30		90		-
6	3	3.8	32 - 50	3	30 ± 4		90		-
7	3	3.8	32 - 50	20	4 ± 1		80		-
8	1.5	1.9	32 - 50	10	4 ± 1			2.1	-
9	7.5	9.5	32 - 50	10	20 ± 3			2.1	-
10	10	12.7	32 - 50	10	38 ± 4			3.0	-
11	3	3.8	20 - 32	5	3 ± 1	3.6			-
12	3	3.8	32 - 50	5	8 ± 1	3.4	40	2.1	0.66
13	3	3.8	50 - 60	5	17 ± 2	3.1			-
14	3	3.8	60 - 80	5	38 ± 4	4.3			-
15	3	3.8	32 - 50	3	10 ± 1		30		1.05
16	3	3.8	32 - 50	7.5	5 ± 1		38		0.50
17	3	3.8	32 - 50	10	3.5 ± 1		35		0.39
18	5	6.3	32 - 50	5	12 ± 2			1.9	1.10
19	7.5	9.5	32 - 50	5	21 ± 3			2.2	1.65
20	10	12.7	32 - 50	5	32 ± 4			2.5	2.20

In column 7, 8 and 9 of table IV the proportionality has been verified between the N value and respectively r_o^2, v^{-1} (or R^{-1}) and h as required by equation (13). It appears that the latter describes quite well the influence of flow rate and column height. While the dependence upon r_o^2, especially for smaller particle size (and than still only for Cs) shows some significant deviation from the proposed law. This may probably be attributed to the irregularity of the characteristics of the crushed particles as compared to nice spheres and to some extent to the rather poor accuracy of the graphical determination of N values above 100.

Applying equation (13) we have calculated some N values of the breakthrough curves using the basic data Kd, D and $\bar{D}$ resulting from "fractional equilibrium" experiments. Column 10 of table IV shows the results and points at the fact that a rough proportionality exists between the graphical determination of N and its theoretical counterpart. The mean reason for the discrepancy lies in the variation of $\bar{D}$ and $\frac{C}{\bar{C}}$ with the degree of occupancy of the exchanger. Glueckauf's formula (12) was indeed derived for saturation conditions where the latter mentioned parameters remain constant.

CONCLUSIONS

The analysis of the kinetic experiments and column runs has shown that in most exchange reaction the rate determining steps vary according to the degree of saturation. At very low loading the diffusion through the film is the main mechanism and at almost saturation,particle diffusion is the controlling step.In between there is a large gap where both mechanisms interfere.

The half time of the exchange reaction varies linearly with the distribution coefficients in film diffusion whereas no explicit function for particle diffusion could be derived.

The accessibility of FeMo varies with the contact time in solution
weakening the structure of the exchanger and making it more open for
the exchanging ions. Between the experimental breakthrough curves
characterized by the dimensionless parameter N (according to the
VERMEULEN HIESTER approach) and the calculated N values derived
from the exchange data and diffusion constants (according to GLUECKAUF
expression) there is a rough proportionality.
However the principle of the latter approach has been proved to be
valid since good agreement was found between the column capacity
parameter N and the physical variables the square of the particle
radius (r_o^2), the flow rate (R: cm^3/sec) and the height of the
column h (cm).

NOTATION

A	= cation initially on the ion exchanger
B	= cation initially in solution
$\bar{C}_A$, $\bar{C}_B$	= the relative concentrations of the ionic species on the exchanger
$\dfrac{\bar{C}}{C}$	= ratio of the sorbed quantity of ion species per ml of ion exchanger to the concentration of the same ions per ml of solution.
D_A , D_B	= ion diffusivities in aqueous solution cm^2/sec.
$\bar{D}_A$, $\bar{D}_B$	= ion diffusivities in ion exchanger, cm^2/sec.
$\bar{D}_{AB}$	= interdiffusion coefficient, sq.cm/sec; first letter of subscript indicates ion initially on exchanger.
$\bar{D}_{AB}$	= mean value of $\bar{D}_{AB}$ throughout the whole ion exchange reaction, cm^2/sec
fe	= fractional void volume in ion exchange particles.
H	= effective height of theoretical plate, see $\underline{/}6\underline{/}$, cm.
h	= column height, cm
Kd	= ratio of the sorbed quantity of ions per gram of ion exchanger to the concentration of the same ions per ml of solution, ml/g
N	= number of effective plates in column operations, see $\underline{/}16\underline{/}$
n	= integer used in summation terms
R	= volumetric flow rate, cm^3/min
r_o	= mean particle radius, cm
T	= contact time, min
$t_{1/2}$	= time interval between the beginning of the ion exchange reaction and the moment when it has reached 50°/o conversion, sec or min
$t_{1/2}^{exp}$	= experimental determined $t_{1/2}$ value, sec. or min
$t_{1/2}(v=\infty)$	= $t_{1/2}$ value for $\left(\dfrac{1}{1 + 70\, r_o\, v} \right) = 0$, sec or min
$U(t)$	= fractional attainment of ion exchange equilibrium
V	= volume of a well weighted quantity of ion exchange materials, cm^3
v	= linear flow rate of percolating solution, cm/sec
z_A , z_B	= ionic valency

α_B^A = separation factor

ΔV = volume increase of a certain volume of ion exchange material, cm^3

ΔV_{max} = maximum volume increase of a certain volume of ion exchange material, cm^3

δ = film thickness, cm

τ = $\dfrac{\overline{D}_{AB} t}{r_o^2}$ equation (2)

Literature cited

/1 _/ A.W.ADAMSON and J.J.GROSSMAN
J.Chem.Phys., 17, 1002 (1949)

/2 _/ L.H.BAETSLE, D.VAN DEYCK, D.HUYS and A.GUERY
III.Int.Conf.on the peaceful Uses of At.En.
Geneva, Paper 28/P/772 (1964)

/3 _/ L.H.BAETSLE, D/VAN DEYCK and D.HUYS
J.Inorg.Nucl.Chem., 27, 683 (1965)

/4 _/ L.H.BAETSLE, D.VAN DEYCK and D.HUYS
paper in preparation.J.Inorg.Nucl.Chem.

/5 _/ G.E.BOYD, A.W.ADAMSON and L.S.MYERS Jr
J.Am.Chem.Soc.,69,2836 (1947)

/6 _/ E. GLUECKAUF
"Ion Exchange and its Applications" edited by the Soc.of
Chem.Industry, London, (1955) p.34.

/7 _/ J.J.GROSSMAN and A.W. ADAMSON
J.Phys.Chem. 56, 97, (1952)

/8 _/ F.HELFFERICH and M.S. PLESSET
J.Chem.Phys., 28, 418 (1958)

/9 _/ F.HELFFERICH
Ion Exchange, Mc Graw-Hill,Book Company,Inc.(1962)p.275

/10_/ F.HELFFERICH
J.Chem.Phys., 38, 1688 (1963)

/11_/ B.HERING and H.BLISS
A.I.Ch.E.Journ. 9, 495 (1963)

/12_/ D. HUYS and L.H.BAETSLE
J.Inorg.Nucl.Chem., 26, 1329 (1964)

/13_/ A.OPLER and N.K. HIESTER
Tables for predicting the performance of fixed bed ion exchange
and similar mass transfer processes.
Stanford Research Institute,Stanford,California (1954)

/14_/ M.S.PLESSET, F.HELFFERICH and J.N. FRANKLIN
J.Chem.Phys., 29, 1064 (1958)

/15_/ R.SCHOGL and F.HELFFERICH
J.Chem.Phys., 26, 5 (1957)

/16_/ Th.VERMEULEN
Advances in Chemical Engineering Vol II p 147-208 (1958)
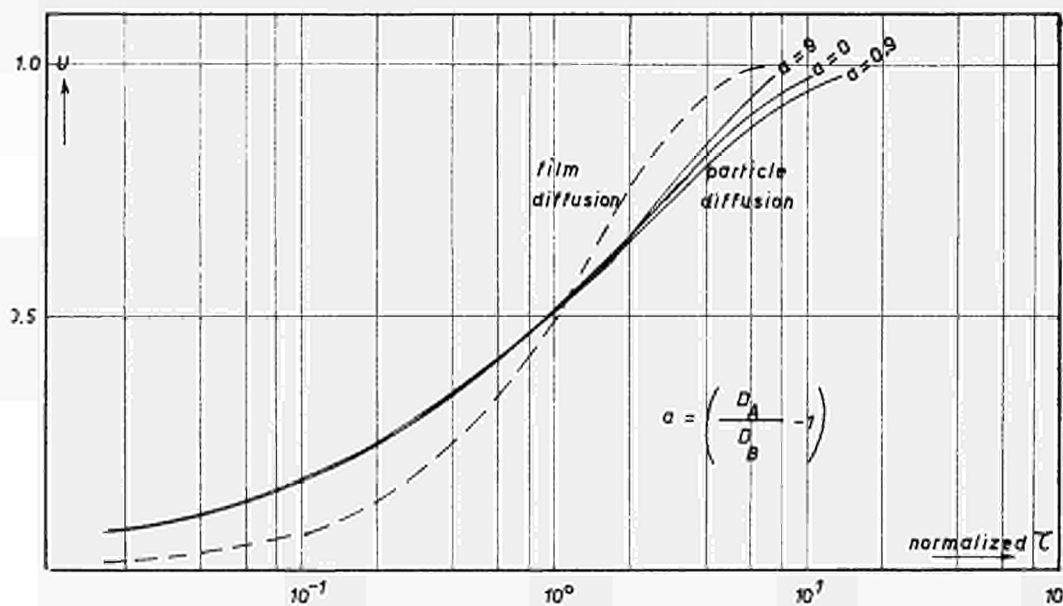
FIG.1 – THEORETICAL CURVES GIVING THE FRACTIONAL ATTAINMENT OF
EQUILIBRIUM AS A FUNCTION OF NORMALIZED TIME FOR
DIFFERENT D_A/D_B RATIOS

$$a = \left(\frac{D_A}{D_B} - 1 \right)$$

A   Solution tank
B   Scintillation crystal
C   Photo multiplier tube
     assembly and preamplifier
D   Lead shield
E   Thermometer
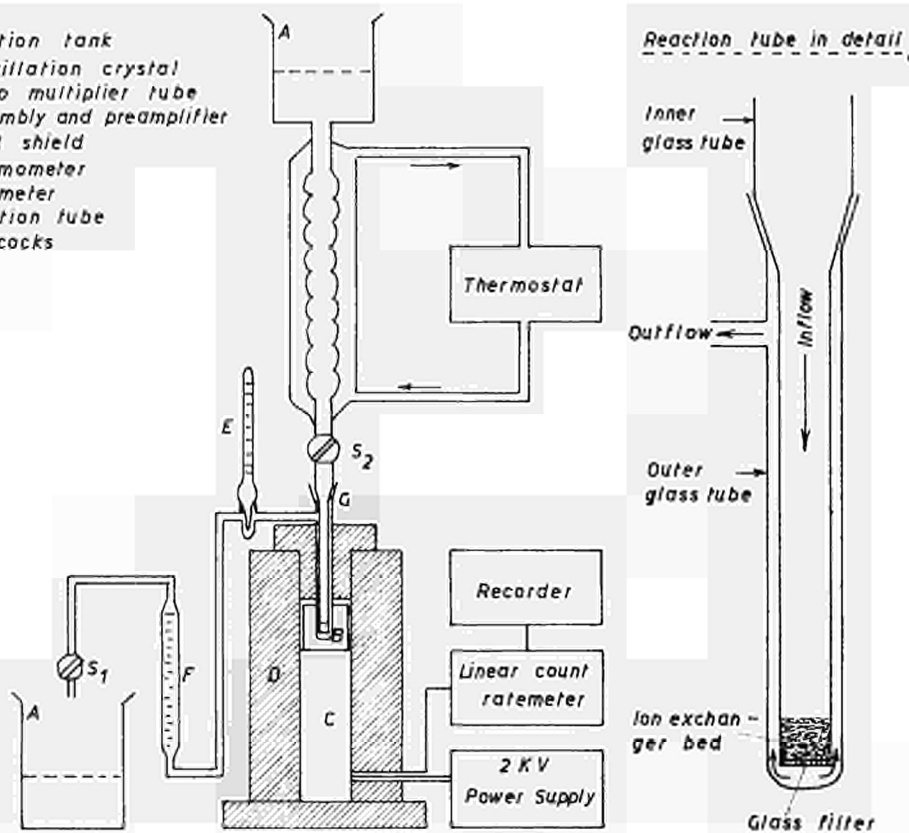F   Flowmeter
G   Reaction tube
$S_1 S_2$ Stopcocks

Reaction tube in detail

FIG.2 – EXPERIMENTAL ARRANGEMENT USED TO OBTAIN KINETIC DATA
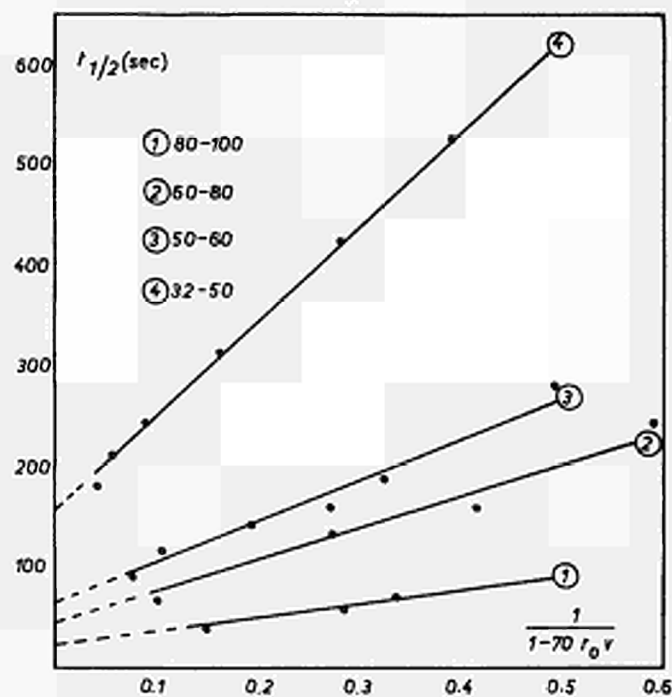
FIG. 3 – INFLUENCE OF FLOW RATE UPON ION EXCHANGE REACTION RATE
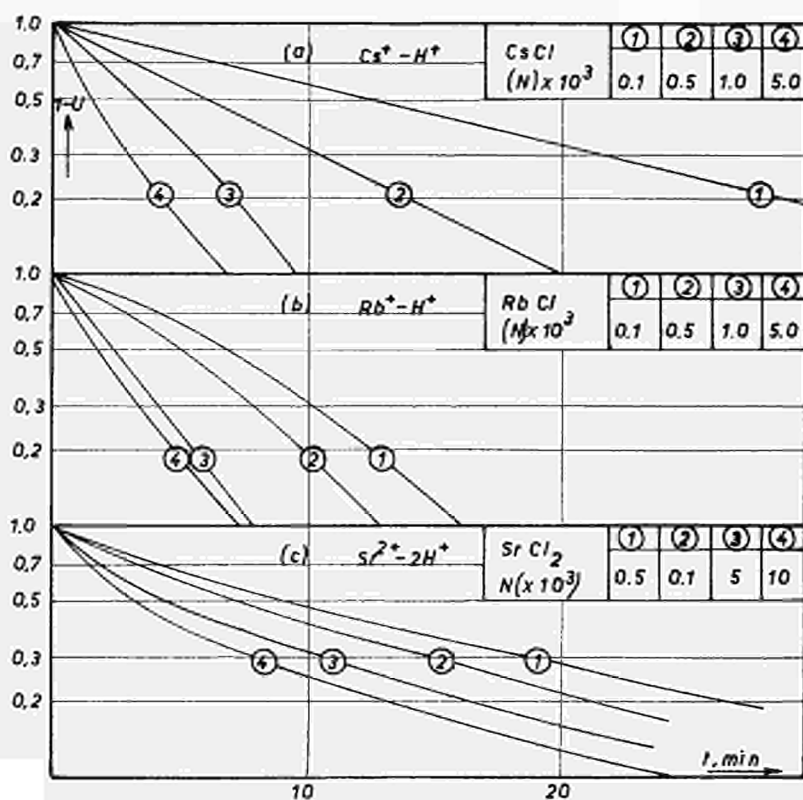
FIG. 4 – INFLUENCE OF ION CONCENTRATION UPON REACTION RATES
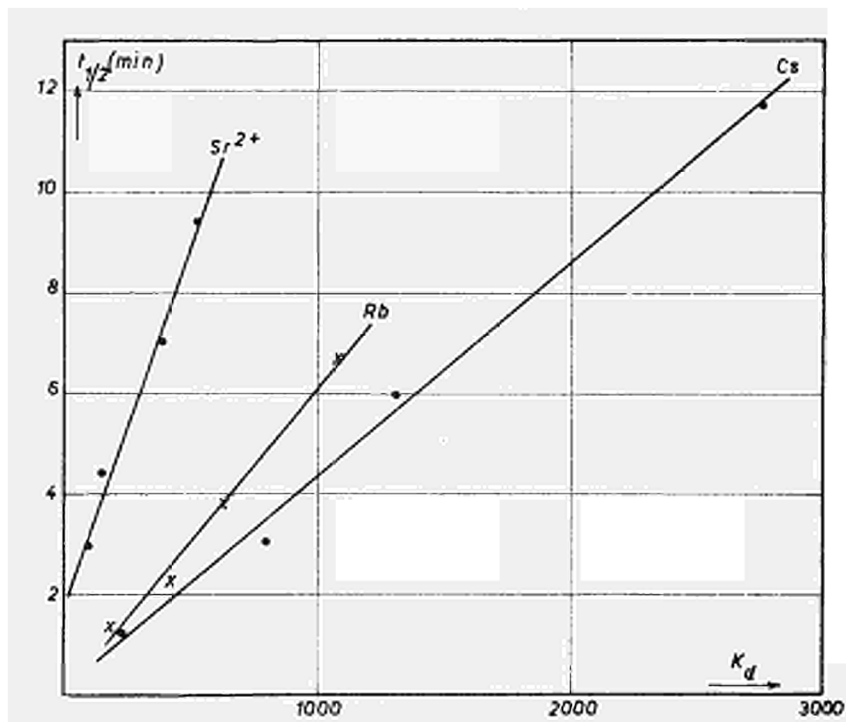
FIG. 5 - DEPENDENCE OF $t_{1/2}$ UPON K_d VALUE
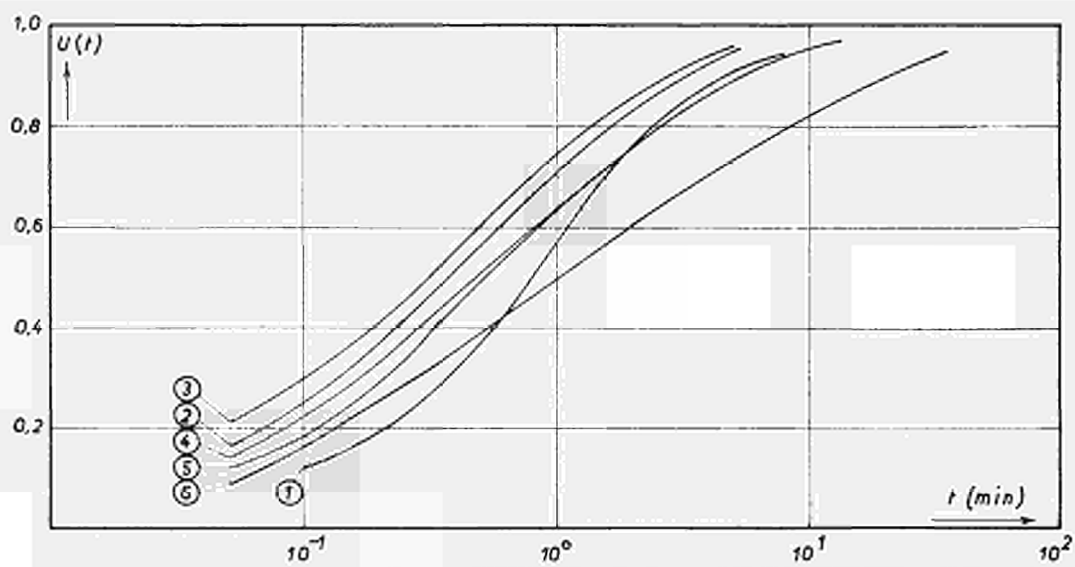
	①	②	③	④	⑤	⑥
$(N)_{CsCl} \times 10^2$	1	3	5	7	9	9,9
$(N)_{HNO_3} \times 10^2$	9	7	5	3	1	0,1

FIG. 6 - DEPENDENCE OF REACTION RATE UPON CONCENTRATION RATIO OF
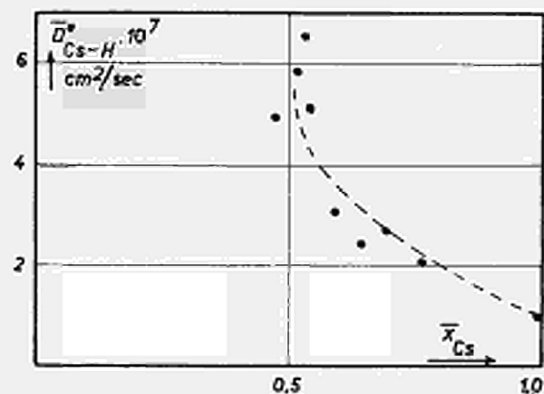EXCHANGING IONS. $(Cs^+ - H^+)$

FIG.7 - DEPENDENCE OF THE "MEAN" INTERDIFFUSION COEFFICIENT
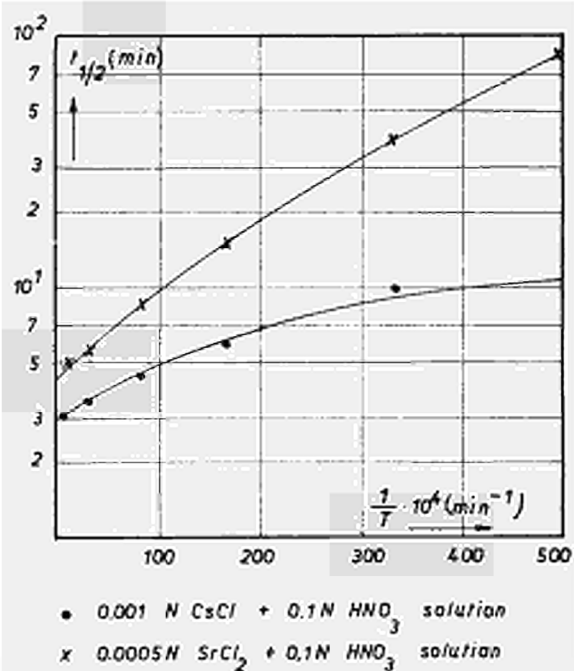
UPON ACHIEVED DEGREE OF CONVERSION. ($Cs^+ - H^+$)

- 0.001 N CsCl + 0.1N HNO_3 solution

x 0.0005N $SrCl_2$ + 0.1N HNO_3 solution

FIG.8 - INFLUENCE OF CONTACT TIME (T) UPON REACTION
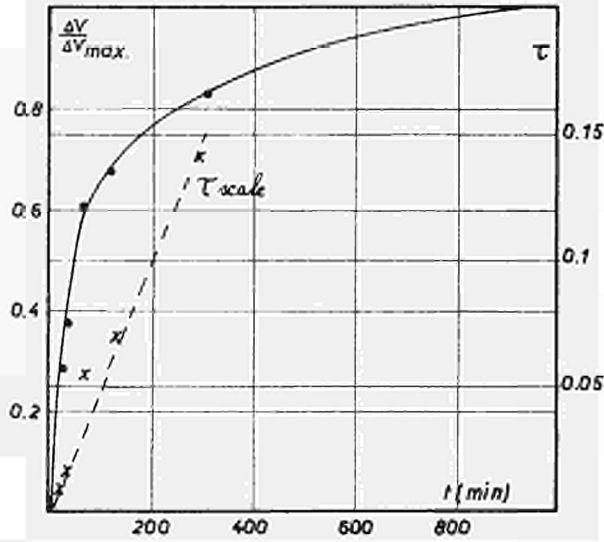
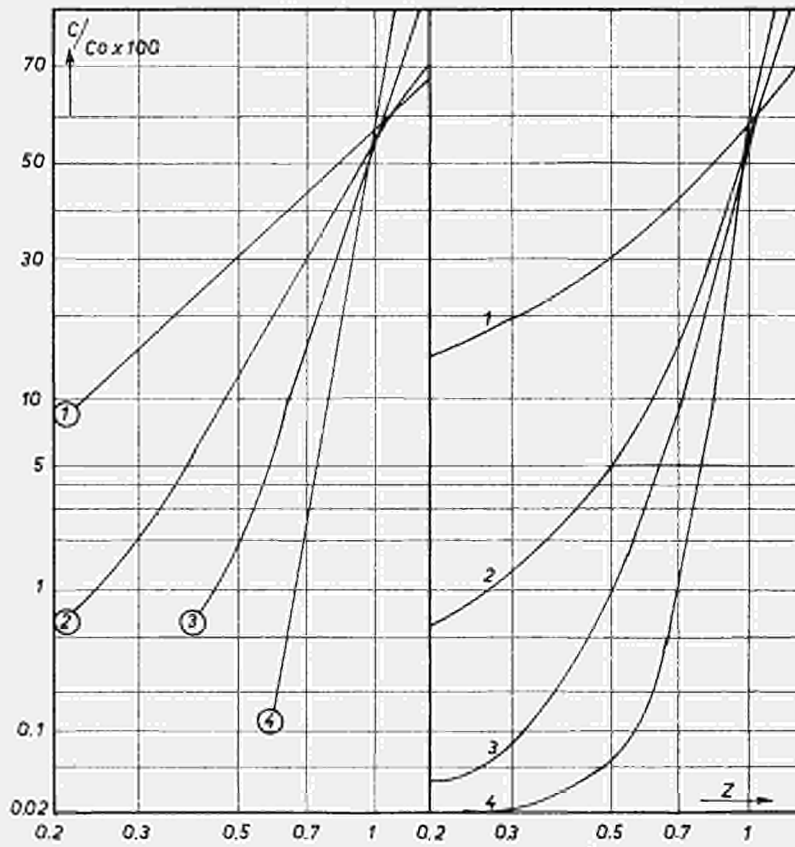KINETIC BEHAVIOUR OF FEMO

FIG. 9 - RATE OF RELATIVE SWELLING OF FeMo IN ACID SOLUTION

(0.1 N HNO$_3$)

Column size : (1.05 x 4.5) cm^3

Weight of ion exchanger : 5 g FeMo

Solution: 500 ppm Cs$^+$ in 2M HNO$_3$

Temperature : 25°C

Flow rate: ① : 20 ml/min

② : 10 ml/min

③ : 3 ml/min

④ : 1 ml/min

Particle size: 32-50 mesh ASTM

Solution: 200 ppm Sr^{2+} in 0.2M HNO$_3$

Temperature : 25°C

Flow rate: 5 ml/min

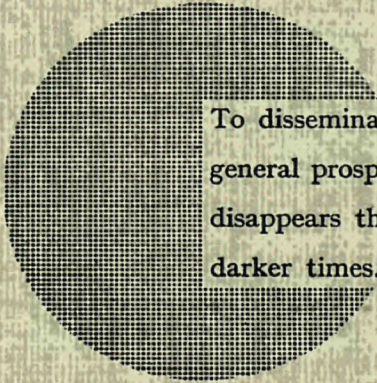1   20-32 mesh ASTM

2   32-50 mesh ASTM

3   50-60 mesh ASTM

4   60-80 mesh ASTM

FIG. 10a - INFLUENCE OF FLOWRATE UPON

BREAKTHROUGH CURVES

FIG. 10b - INFLUENCE OF PARTICLE SIZE

UPON BREAKTHROUGH CURVES

To disseminate knowledge is to disseminate prosperity — I mean general prosperity and not individual riches — and with prosperity disappears the greater part of the evil which is our heritage from darker times.

Alfred Nobel

SALES OFFICES

All Euratom reports are on sale at the offices listed below, at the prices given on the back of the cover (when ordering, specify clearly the EUR number and the title of the report, which are shown on the cover).

PRESSES ACADEMIQUES EUROPEENNES

98, Chaussée de Charleroi, Bruxelles 6

Banque de la Société Générale - Bruxelles
compte Nº 964.558,

Banque Belgo Congolaise - Bruxelles
compte Nº 2444.141,

Compte chèque postal - Bruxelles - Nº 167.37,

Belgian American Bank and Trust Company - New York
compte No. 22.186,

Lloyds Bank (Europe) Ltd. - 10 Moorgate, London E.C.2,

Postcheckkonto - Köln - Nr. 160.861.

OFFICE CENTRAL DE VENTE DES PUBLICATIONS DES COMMUNAUTES EUROPÉENNES

2, place de Metz, Luxembourg (Compte chèque postal Nº 191-90)

BELGIQUE — BELGIË
MONITEUR BELGE
40-42, rue de Louvain - Bruxelles
BELGISCH STAATSBLAD
Leuvenseweg 40-42 - Brussel

DEUTSCHLAND
BUNDESANZEIGER
Postfach - Köln 1

FRANCE
SERVICE DE VENTE EN FRANCE
DES PUBLICATIONS DES
COMMUNAUTES EUROPEENNES
26, rue Desaix - Paris 15e

GRAND-DUCHE DE LUXEMBOURG
OFFICE CENTRAL DE VENTE
DES PUBLICATIONS DES
COMMUNAUTES EUROPEENNES
9, rue Goethe - Luxembourg

ITALIA
LIBRERIA DELLO STATO
Piazza G. Verdi, 10 - Roma

NEDERLAND
STAATSDRUKKERIJ
Christoffel Plantijnstraat - Den Haag

EURATOM — C.I.D·
51-53, rue Belliard
Bruxelles (Belgique)